PERGAMON

Computers and Structures 73 (1999) 373–383

Computers & Structures

www.elsevier.com/locate/compstruc

Inelastic stability of rectangular frames by transfer matrices

E.S. Kameshki [a,*], S. Syngellakis [b]

[a] Department of Civil and Architectural Engineering, University of Bahrain, PO Box 32038, Isa Town, Bahrain
[b] Department of Mechanical Engineering, University of Southampton, Southampton, SO17 1BJ, UK

Received 8 November 1996; accepted 26 June 1998

Abstract

A formulation of the stability problem for tall unbraced frames, deformed beyond their elastic limit, has been developed using transfer matrices. A linear incremental solution procedure allows the monitoring of plastic hinge formation and the resulting reduction of the member stiffness until the critical load is located. The most important second order effects arising from large deformation have been accounted for. Simple modeling of inelastic behaviour has been adopted although further refinement of the formulation at no significant computational cost is indicated. Extensive application of the developed computer algorithm and comparison of its predictions with other analytical results confirms the validity of the proposed method of solution.

Keywords: Stability; Plastic properties; Frames; Steel; Transfer matrices; Computer applications

1. Introduction

Large axial forces in the stanchions of high-rise buildings generate additional moments and displacements, which may lead to yield, and plastic deformation well before the elastic critical load is reached. The simple plastic theory, based on rigid–perfectly-plastic material behaviour, does not account for precollapse deformation and axial forces, primarily subjected to flexure. However, the ultimate load carrying capacity of multi-storey buildings or any other slender structure subjected to large compressive loads would also depend on the geometric changes arising from deformation. A rational elastic–plastic stability analysis, accounting for the formation of plastic hinges due to yielding and ductility of steel as well as the simultaneous deterioration of the elastic stiffness due to geometric nonlinearity, should lead to a lower collapse load than that predicted by rigid–plastic theory. Experiments have shown that this is actually the case for unbraced, rigidly or semi-rigidly connected tall steel frames.

Extensions of full nonlinear elastic or plastic limit analyses to elasto-plastic range were early proposed and developed [11,16]. Jennings and Majid [6] based their formulation of the overall stiffness matrix on the displacement method. Parikh [14] obtained general slope–deflection equations for different cases of hinge formation in stanchions and girders. Advanced second-order elastic–plastic analysis incorporated the effects of axial deformation [10,14], bowing [9], as well as spread of plastic zone and strain reversal [1]. McNames and Lu [13] developed a formulation which relies on small fictitious lateral force acting on the frame with the buckling load obtained by extrapolation. Their predictions were verified experimentally. Analyses based on the concepts of minimum complementary energy [3] and virtual work [2] incorporated the effects of axial deformation and spread of plastic zone, respectively.

* Corresponding author.

0045-7949/99/$ - see front matter
PII: S0045-7949(98)00273-9

Nomenclature

c	stability function
$\mathbf{d}$	displacement vector
E	Young's modulus
$\mathbf{G}$	field transfer matrix
g	external joint movement
I	second moment of cross sectional area
K	elasto-plastic stiffness coefficient
L	beam element length
M	number of stanchions
m	moment
N	number of storeys
P	member axial force (positive if compressive)
P	axial force
$\mathbf{p}$	force vector
Q	force vector in field equation
q	shear force
$\mathbf{R}$	force vector in station equation
$\mathbf{r}$	external force vector
$\mathbf{S}$	state vector
s	stability function
U	station transfer matrix
u	axial displacement
v	lateral displacement
Z	plastic section modulus
δ	small increment symbol
Δ	v_2-v_1, storey (member) sway
θ	rotation (positive counter-clockwise)
λ	load factor
ρ	ratio of lateral to vertical load

Subscripts

c	critical
p	plastic

Superscripts

I	floor index
i	storey index
J	girder index
j	stanchion index
r	reference stanchion
t	transpose of a matrix

Other work has focused on the reduction of the plastic moment of a section due to the presence of axial force [5,7]. Finite element analyses [4,8,17] have accounted for gradual yielding of cross section strain hardening, residual stresses as well as connection flexibility.

The analysis and numerical algorithm presented in this paper is sufficiently rigorous to yield accurate predictions of elasto-plastic frame behaviour without excessive demands on computer time and memory. It is based on the transfer matrix method, which is applicable to structures modelled as single, nonbranching chain members. Whereas classical stiffness matrix formulation involves all the global degrees of freedom of a structure, transfer matrix solutions on those of the substructure generated by the modelling. Considerable condensation of the problem is thus directly achieved. A stability analysis of this type has already been developed for the elastic frames [15] which is here extended to the elasto-plastic range by introducing sensible and well tested models for the reduced stiffness of members due to plastic hinge formation.

2. Theory

The analysis is restricted to plane frames with buckling occurring in the plane of the frame, that is, any out-of-plane movement inhibited. Members are assumed to be straight, prismatic, inextensible and symmetric with respect to the x–y plane which coincides with the plane of the frame. The material is assumed to be elastic–perfectly plastic, that is, strain hardening is ignored. With both stanchions and girders deforming in double curvature, plastic hinges are anticipated at the ends of members. Furthermore, due to gravity loading, plastic hinges are also expected to form at some point within the span of girders. The effect of spread of plasticity on the stability behaviour has been found to be small for frames up to a certain size [4,8]; therefore, within properly assessed limits, localized plasticity can be applied with the confidence that it would lead to sufficiently accurate results.

In the course of analytical formulation and its computer implementation, it was found that, if plastic hinges are not allowed to form at the ends of stanchions, the capacity of the method to predict the failure mode is reversly restricted. In order to avoid the numerical difficulty which may arise from removing this limitation, an assumption, not normally found in conventional elastic–plastic analyses, is adopted here, namely that a plastic hinge can form near the end of a stanchion at a small finite distance from the centre of a joint.

According to the adopted notation, u, v, θ, p, q, m represent the axial displacement, transverse displacement, rotation, axial force, shear force and bending

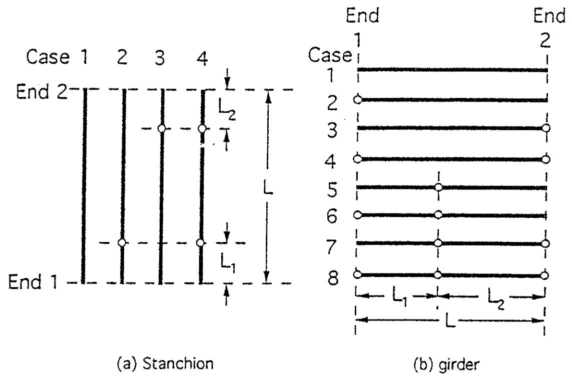

Fig. 1. Plastic hinge combinations in members.

moment of a cross section, respectively. Subscripts 1 and 2 indicate the respective ends of a member. Small increments of these variables are related by the modified slope–deflection equations,

$$\delta m_1 = K_1\delta\theta_1 + K_2\delta\theta_2 + K_3\delta\psi \quad (1)$$

$$\delta m_2 = K_4\delta\theta_1 + K_5\delta\theta_2 + K_6\delta\psi \quad (2)$$

with

$$\psi = \frac{\Delta}{L} = \frac{v_2 - v_1}{L} \quad (3)$$

where δ denotes increment of the prefixed quantity, L is the length of the beam, while K_n, $n = 1, \ldots, 6$, are the stiffness coefficients depending on the axial force intensity and the state of elasto-plastic deformation.

Various plastic hinge combinations considered in both stanchions and girders are shown diagramatically in Fig. 1. Slope–deflection equations for all those cases have been derived following a procedure similar to that adopted by Parikh [14]. Written in terms of incremental quantities, they reduce to the form of Eqs. (1) and (2) assuming however that, within a small load step, the variation of their coefficient due to nonlinear deformation or to changes in axial forces is negligible compared to that of the kinematics variables. It is noted that K_n always satisfies

$$K_2 = K_4 \quad (4a)$$

$$K_3 = -(K_1 + K_2) \quad (4b)$$

$$K_6 = -(K_4 + K_5) \quad (4c)$$

thus allowing all subsequently derived expressions to be written in terms of only K_1, K_2 and K_5.

The required elasto-plastic stiffness coefficients for stanchions and girders are assembled in Tables 1 and 2, respectively. The various geometric and material parameters appearing in these tables are defined by

$$c' = 1 - c^2, \quad c'' = 1 + c$$

$$k = \frac{EI}{L}, \quad f = \frac{1}{ksc'}$$

$$\xi_\alpha = \frac{L_\alpha}{L}, \quad \alpha = 1,2$$

$$D = \xi_1^2 f_1 + \xi_2^2 f_2 - PL\xi_1\xi_2 f_1 f_2$$

where $P = p_1 = -p_2$ is the member axial force taken positive if compressive, E the Young's modulus, I the second moment of cross sectional area, while $s(\alpha)$, $c(\alpha)$ are the familiar stability coefficients [12], depending on the parameter

$$\alpha = (PL/4K)^{1/2}$$

Subscripts 1 and 2, attached to the stiffness parameter k, the flexibility parameter f and the stability coefficients, indicate that these quantities are evaluated using beam lengths L_1 and L_2, respectively.

Eqs. (1) and (2) are combined with incremental form of the equations of equilibrium,

$$\delta q_1 + \delta q_2 = 0 \quad (5)$$

$$\delta m_1 + \delta m_2 - L\delta q_1 - p\delta\Delta - \delta p\Delta = 0 \quad (6)$$

It is noted that member axial and shear strain has been neglected but the change in member geometry has been accounted for. Through a series of algebraic operations, it is possible to transform Eqs. (1), (2), (5) and (6) into

Table 1
Elasto-plastic stiffness coefficients for stanchions

Case	K_1	K_2	K_5
1	ks	ksc	Ks
2 and 3	$\frac{\xi_1}{D}(\xi_1 - PL\xi_2 f_2)$	$\frac{\xi_1\xi_2}{D}$	$\frac{\xi_2}{D}(\xi_2 - PL\xi_1 f_1)$
4	$-\frac{PL\xi_1(1-\xi_2)}{1-\xi_1-\xi_2}$	$-\frac{PL\xi_1\xi_2}{1-\xi_1-\xi_2}$	$-\frac{PL\xi_2(1-\xi_1)}{1-\xi_1-\xi_2}$

Table 2
Elasto-plastic stiffness coefficients for girders

Case	K_1	K_2	K_5
1	ks	ksc	Ks
2	0	0	$\frac{1}{f}$
3	$\frac{1}{f}$	0	0
4 and 8	0	0	0
5	$\frac{\xi_1}{D}(\xi_1 - PL\xi_2 f_2)$	$\frac{\xi_1\xi_2}{D}$	$\frac{\xi_2}{D}(\xi_2 - PL\xi_1 f_1)$
6	0	0	$-\frac{PL\xi_2}{(\xi_1 - PL\xi_2 f_2)}$
7	$-\frac{PL\xi_1}{(\xi_2 - PL\xi_1 f_1)}$	0	0

$$\delta\theta_2 = \frac{K_1}{K_2}\delta\theta_1 + \frac{1}{K_2}\delta m_1 + \left(1 + \frac{K_1}{K_2}\right)\delta\psi \tag{7}$$

$$\delta m_2 = AL(-\delta\theta_1 + \delta\psi) + \frac{K_5}{K_2}\delta m_1 \tag{8}$$

$$\delta\psi = \frac{1}{C}(A\delta\theta_1 + \delta q_1 - B_1\delta m_1 - \psi\delta P) \tag{9}$$

$$\delta q_1 = -A\delta\theta_1 + B_1\delta m_1 + C\delta\psi + \psi\delta P \tag{10}$$

$$\delta q_2 = -A\delta\theta_2 + B_2\delta m_2 + C\delta\psi + \psi\delta P \tag{11}$$

where

$$A = \frac{K_1 K_5 - K_2^2}{LK_2} \tag{12a}$$

$$B_1 = \frac{K_2 + K_5}{LK_2} \tag{12b}$$

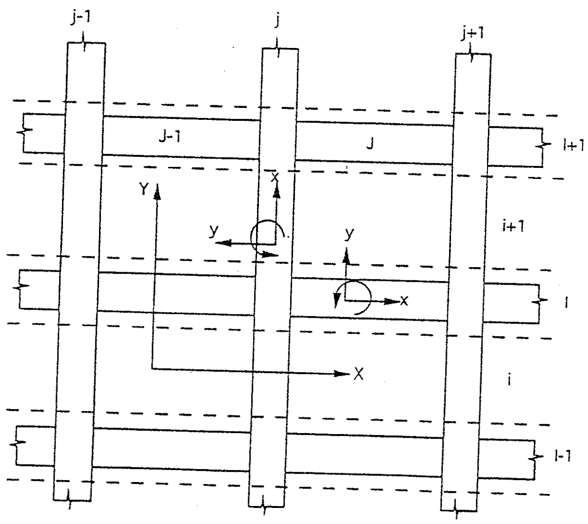

Fig. 2. Structural discretization with frames of reference.

$$B_2 = \frac{K_1 + K_2}{LK_2} \tag{12c}$$

$$C = A + P \tag{12d}$$

As has been pointed out [15], transfer matrices can be assembled for the present problem using Eqs. (7)–(11) applied to all individual girders and stanchions.

3. Transfer matrices

In the present transfer matrix formulation, a member is defined as the combination of all stanchions between two successive floor levels while a joint consists of all interconnecting girders and their physical connections to the stanchions at any floor level. Lower case superscripts denote the storey and stanchion number to which a stanchion element belongs while upper case superscripts were used for the bay and floor number of a girder. The storey, bay floor and stanchion numbering is clearly indicated in Fig. 2 where the orientation of local and global frames of reference are also shown.

According to these definitions and notations, the displacement vector of member i would normally consist of the displacement vectors of all stanchions making up a member. The assumption however of neglecting the axial strain of both stanchions and girders reduces significantly the number of kinematic variables and hence the size of the problem as it leads to the conditions,

$$u^{ij} = 0, \quad V^{ij} = V^i \tag{13}$$

for all $i = 1, \ldots, N$ and $j = 1, \ldots, M$, where N is the number of storeys and M the number of stanchions. Hence, the deformation vector reduces to

$$d^i = \{v^i \quad \theta^{i1} \quad \theta^{i2} \ldots \theta^{iM}\}^t \tag{14}$$

where the superscript t denotes the transpose of an array. By analogy, the force vector should also consist of $M + 1$ elements

$$p^i = \{q^{ir} \quad m^{i1} \quad m^{i2} \ldots m^{iM}\}^{\mathrm{t}} \tag{15}$$

with only one, termed the reference, column contributing a shear force component. This is indicated by the superscript 'r' and is usually chosen to be the stiffest column. With the transfer matrix solution performed at each load step, the state vector

$$S^i_\alpha = \{\delta d^i_\alpha \quad (-1)^\alpha \quad \delta p^i_\alpha\}^{\mathrm{t}} \tag{16}$$

is here defined in terms of the incremental deformation and load vectors.

The next objective is to obtain one set of relations between the state vectors at the two ends of a member and then another between the state vectors at either side of a joint. The first set is formulated by using relations (7)–(10), applied to all individual stanchion segments making up member i and taking into account the condition

$$\Delta^{ij} = \Delta^{ir} = \Delta^i \tag{17}$$

which is the consequence of neglecting axial deformation in the girders. For the derivation of the second set, the compatibility conditions and the equilibrium equations at a typical joint I are combined with Eqs. (1) and (2), applied to all girders belonging to joint I. The slope-deflection equations for girders are written with zero lateral sway as a consequence of neglecting axial deformation in the stanchions.

Apart from the internal forces and moments transmitted by the adjacent beam elements, the external lateral force and moment acting on junctions of 'joint' I and stanchion j, denoted by r^{Ij} and g^{Ij}, receptively, also contribute to equilibrium. It is noted that fixed-end moments from girders with in-span loading, which contribute to g^{Ij}, are affected by plastic hinge formation. Their expressions have been derived in the cases of uniformly distributed load and mid-point load for all the hinge combinations of Fig. 1b. Since the axial load in the girders does not increase significantly, its effect on fixed-end moments has been ignored.

The process of derivation of the various relations between the elements of the state vectors is very similar to that applied in the purely elastic version of the present analysis which has been described in detail [15]. Hence, only the final form of these equations is given in Appendix A. They are grouped into two systems the matrix form of which is

$$S^i_2 = G^i S^i_1 - Q^i \tag{18}$$

$$S^i_1 = U^I S^i_2 - R^I \tag{19}$$

where G^i and U^I are the field and station transfer matrices of the problem, respectively. Vector Q^i is generated by the term $\psi\delta P$ which also contributes to R^I, the external force vector at joint I.

4. Numerical algorithm

Due to the nonlinearity of the problem the solution is performed in small steps. Each step comprises the following numerical tasks:

1. At the beginning of a new step, the load factor is increased by a small amount $\delta\lambda$ and the current properties of the structure as well as the axial forces in all elements are assumed constant. The standard transfer matrix procedure is then carried out using Eqs. (18) and (19) and the appropriate boundary conditions [15]. This yields the incremental state vectors at all levels but also, through further application of the joint equilibrium conditions, the axial forces in all members. On the very first application of the method, the structure is assumed elastic and the axial forces zero.
2. The bending moments at all locations where a plastic hinge is expected to develop are calculated and compared with the plastic moments of the respective sections. If a plastic hinge is formed, the load increment is reduced by a certain factor and the member stiffness is modified according to the relevant slope–deflection relations.
3. The initial solution can be improved to reflect the change in the axial forces and member stiffness within the current step. This is achieved through an iterative scheme whereby the transfer matrix solution is repeated until satisfactory convergence of forces or displacements is reached. The standard procedure is only slightly modified to account for the non-vanishing vector Q appearing in Eq. (18).
4. The determinant of the coefficients of the solution matrix is computed and compared with that obtained at the end of the previous step. It is worth noting that the order of this determinant is $(M+1)\times(M+1)$. If a change of sign is observed, a singularity has been detected which can lead to the critical load. If the current step is the first one, then the solution moves directly to the second step.
5. If the solution determinant does not change sign, the total current force and displacement components are calculated by adding their increments, obtained through tasks 1–3, to their previous values. The solution can then proceed to its next step.

The above procedure is repeated until the determinant becomes singular as a consequence of loss of stability or formation of a plastic collapse mechanism. At this instant the analysis is terminated and the total applied load is the failure load of the structure.

Table 3
Properties of symmetric, single-bay frames

Frame no.	Storey no.	Stanchions I (cm^4)	Stanchions Z (cm^3)	Girders I (cm^4)	Girders Z (cm^3)	Girders Depth (cm)
1	1	27,596	1926	21,561	1179	40.7
	2–4	14,193	1207	51,561	1179	40.7
2	1	66,306	3977	69,706	3376	46.1
	2	614,465	3702	56,404	3048	41.5
	3	52,716	3212	50,888	2769	41.0
	4	52,716	3212	38,643	2383	36.0
	5	52,716	3212	35,430	2196	35.7
	6	38,643	2383	33,165	2058	36.0
	7	33,165	2058	26,701	1678	35.3
	8	26,701	1678	26,701	1678	35.3
	9	19,817	1418	22,564	1427	35.4
	10	16,420	1190	14,601	1064	30.6
	11	12,907	944	11,688	842	31.1
	12	8728	770	11,688	842	31.1
	13	8728	770	8495	623	30.4
	14	4071	444	5544	483	25.6
	15	2348	259	2880	313	20.7

5. Results

A FORTRAN code was developed for implementing and testing the analysis. It allows for variation of dimensions and loading with height as well as any type of support condition. Lateral as well as gravity concentrated or distributed load can be applied to stanchions and girders, respectively. The code does not include iteration within each load step relying rather on small load increments for accuracy. This implies constant axial load within each step and obviates the need to include vectors Q in the formulation. At this stage of its development, the computer program has two more limitations, namely that inelastic strain reversals caused by unloading at plastic hinges are not anticipated and that the reduction of plastic moment in stanchions due to the presence of axial forces has not been taken into account.

Table 4
Sectional properties of the double-bay frame

Storey no.	Stanchions No.	Stanchions I (cm^4)	Stanchions Z (cm^3)	Girders Bay no.	Girders I (cm^4)	Girders Z (cm^3)	Girders Depth (cm)
1	1	10,348	901	1	8495	623	30.4
	2	19,817	1417	2	5544	484	25.6
	3	5265	569				
2	1	6089	654	1	8495	623	30.4
	2	11,359	988	2	4425	395	25.1
	3	4566	498				
3	1	4566	498	1	8495	623	30.4
	2	11,359	988	2	2880	313	20.7
	3	2227	311				
4	1	4566	498	1	8495	623	30.4
	2	5265	569	2	2348	259	20.3
	3	2227	311				
5	1–3	2227	311	1	8495	623	30.4
				2	2348	259	20.3
6	1–3	2227	311	1	2880	313	20.7
				2	2348	259	20.3

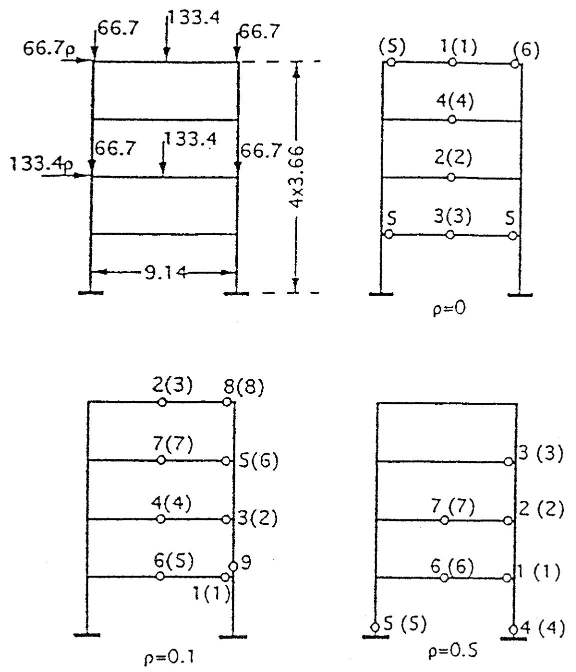

Fig. 3. Example frame 1.

The elasto-plastic slope–deflection equations for stanchions have been applied with the finite distance of a hinge from the centre of a joint taken equal to the adjacent girder half-depth. This choice can be justified as accounting, to a certain extent, for the local stiffening of the stanchion arising from the finite size of its connection with the girder. A more rational choice should be based on a rigorous modeling of the particular connection used and the identification of the most 'critical' section in the stanchion. Provided however that this finite distance is small relative to the storey height, numerical results have shown little sensitivity to its variation; the adopted rough approximation can thus be considered acceptable.

The computer program has been validated through its application to several frames of various sizes the stability of which have been the object of previous investigations. Detailed results are presented here for the three interesting, thoroughly and repeatedly analysed cases providing reliable standards for comparison. The cross sectional properties of these frames are given in Tables 3 and 4 in which Z represents the plastic modulus of the member. Their dimensions and unfactored loading are given in Figs. 3–5 in metres and kilonewtons, respectively. The same lateral and vertical load is applied to all floor levels apart from the top one. A Young's modulus E of 201 GPa was specified for frames 1 and 3 while E = 207 GPa for frame 2. The corresponding values of the yield stress were 236 and

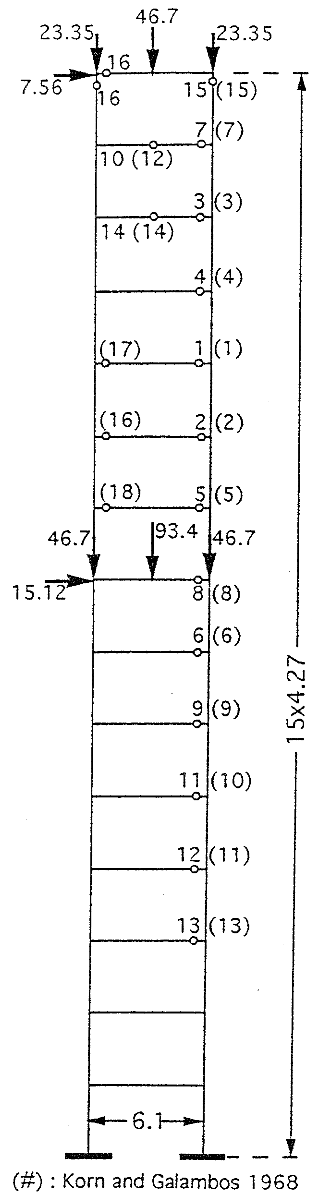

Fig. 4. Example frame 2.

248 MPa. The present predictions of their failure load factor λ_c for various values of $\delta\lambda$ as well as the corresponding published results are collected in Table 5. The order of plastic hinge formation resulting from the present transfer matrix as well as from previous analyses is shown in Figs. 3–5.

The nonlinear lateral deflection of all frames under proportionally increased loading was also assessed and compared to earlier predictions. Results are presented for the extreme case of the 15-storey frame 2, the top sway deflection of which, computed using a load factor

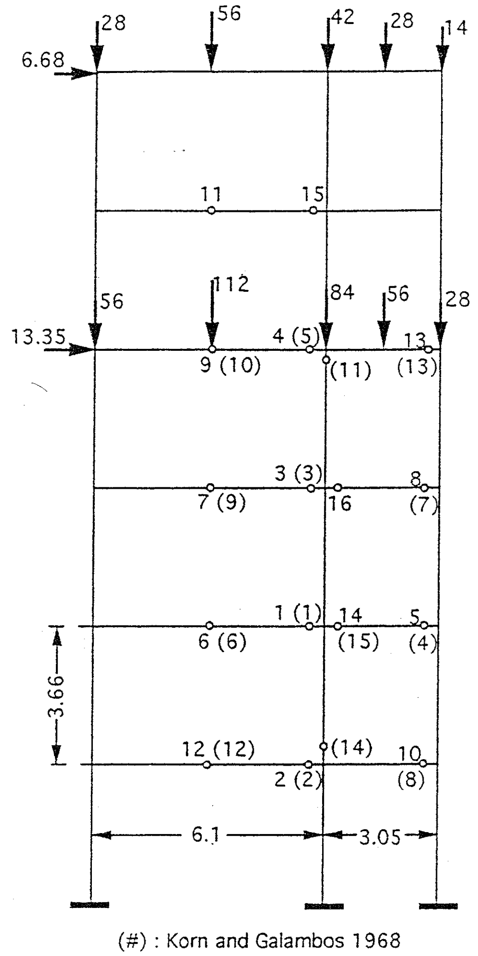

Fig. 5. Example frame 3.

increment of 0.02, is shown in Fig. 6 together with that obtained by Korn and Galambos [11] neglecting axial deformation. The effect of the latter is expected to be significant in a tall, single-bay frame under considerable lateral load. This was confirmed by Korn and Galambos [11] and later by Kassimali [8]. Their almost identical results using analyses that account for axial deformation are also shown in Fig. 6. Omitted second order effects as well as other simplifying assumptions mentioned above may cause wider discrepancy in the elasto-plastic range.

Finally, the efficiency of the computer program was assessed by noting the time for various frame sizes and load factor increments. Run on a micro VAX 2, its more demanding application was that on the 15-storey, single-bay frame using a $\delta\lambda$ of 0.01, which took about 11 min to run. For smaller frames and larger load increments, the execution time was significantly less.

6. Discussion

The transfer matrix solution has been shown to provide satisfactory answers to the inelastic stability problem for plane rectangular frames. It was noted that present and past results for the failure load and lateral deflection were in very good agreement. The small discrepancies may be attributed to the additional second order effects considered by the previous and ignored by the present analysis. As expected, the predictions of the adopted linear incremental solution show some sensitivity to the choice of load increment. For sufficiently low values of the latter however, the failure load converges to a stable limit. The value of the load increment apparently also affects slightly the order of plastic hinge formation at the stages of loading. Referring, in particular, to the frame of Fig. 3, a better agreement of the transfer matrix results with the published predictions [8] was noted when a higher value for $\delta\lambda$ was used.

Discrepancies may also arise from the assumption that the plastic chinge in the stanchion occurs at some finite distance from the joint centre. This expected to delay the prediction of failure but may represent more closely the actual structural behaviour as it accounts indirectly for the stiffening effect of the connection. It is worth assessing the validity of this assumption experimentally or through a more elaborate numerical approach such as a finite element analysis.

The full plastic moment of a section is reduced by the presence of large axial forces in the stanchions. This effects has been shown to be small on the critical load of the analysed frames, but it could be more significant in larger structures. It may also be more important in relation to the sequence of plastic hinge formation and the final mode of failure. Thus, the present analysis predicts a joint collapse mechanism in frames 2 and 3 in contrast to the results of an earlier analysis [11] which accounts for this effect. It was also confirmed that the effect of axial deformation and bowing on failure load and sway deflection is insignificant in low-rise wide frames [4,8,10] but, as already indicated in the previous section, it could be more significant on the sway deflection of tall, narrow frames.

The proposed technique is based on a relatively simple computational procedure, its implementation on the computer follows a more or less standard programming pattern and the resulting code can accept data and yield results quickly. Moreover, a degree of efficiency in computer storage and time is achieved. The present formulation certainly lacks the versatility of a finite element solution but the application of the more widely accessible FE codes to buckling has its limitations arising from the large number of elements required to model nonlinearly deforming members under high axial loads. In contrast, the transfer matrix

Table 5
Failure loads of the analysed frames

Frame no.	Transfer matrices $\delta\lambda$	λ_c	Published results
1 ($\rho=0$)	0.05	1.800	1.828[a]
	0.02	1.828	
	0.01	1.838	
1 ($\rho=0.1$)	0.05	1.687	1.687[a]
	0.02	1.716	
	0.01	1.723	
1 ($\rho=0.24$)	0.05	1.512	1.502[a]
	0.02	1.548	1.501[b]
	0.01	1.608	1.501[c]
			1.556[d]
1 ($\rho=0.5$	0.05	1.075	1.075[a]
	0.02	1.099	
	0.01	1.109	
2	0.05	1.389	1.395[a]
	0.02	1.400	1.403[b]
	0.01	1.426	
3	0.09	1.366	1.367[b]
	0.05	1.395	
	0.01	1.431	

[a] Kassimali, 1983..
[b] Korn and Galambos, 1968.
[c] Korn, 1981.
[d] Gharpuray and Aristizabal-Ochoa, 1989.

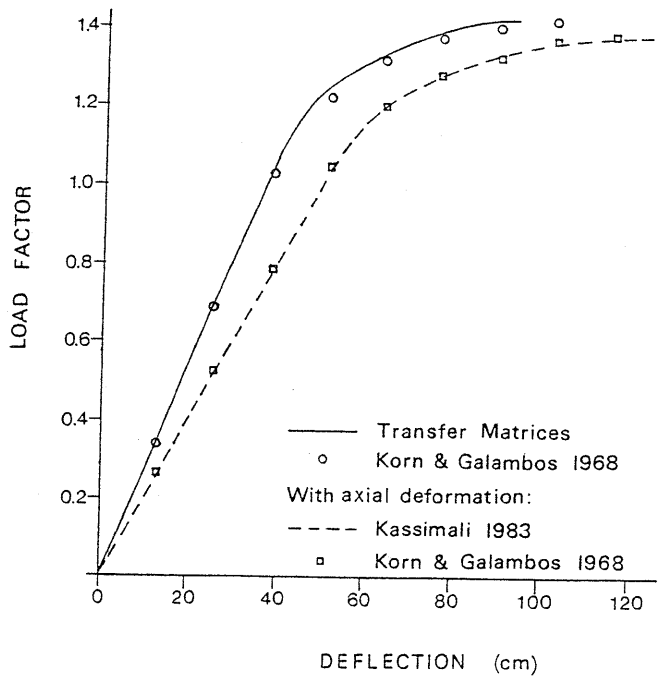

Fig. 6. Top storey sway of frame 2.

approach leads to a substantially lower number of degrees of freedom as well as order of the solution matrix, that is, number of simultaneous equations to be solved. It is also worth noting that the size of the transfer matrices and therefore of the solution matrix remains unchanged even after plastic hinges are formed in members. A limitation of the transfer matrix method arises from accumulation of error due to rounding numbers in the successive multiplications leading to the solution matrix.

As a first step towards further development of the presented numerical algorithm, the dependence of plastic moment on axial force and residual stresses could be accounted for. This can be achieved by substituting the computed axial member forces into existing, reliable, approximate models [8] to update the plastic moment at each load step. The analysis can be easily expanded to include models for semi-rigid connections, spread plasticity and the strain reversals caused by unloading at plastic hinge. Modelling of strain hardening is feasible, since however its effect on frame behaviour is expected to counter that of residual stresses, it is reasonable to assume that accounting for both effects would make a very small difference to the failure load [4]. There is considerable scope in improving the numerical efficiency of the solution algorithm so that it copes with a higher number of bays and storeys.

Extension to more complex geometries that would include bracing and uneven number of stanchions would enhance the versatility of the method.

Acknowledgements

The first author gratefully acknowledges the support of the University of Bahrain during her research programme on the work reported in this paper.

Appendix A

The expanded form of matrix Eq. (18) is:

$$\delta v_2^i = \delta v_1^i + L^i \delta\psi^i \tag{A1}$$

$$\delta\theta_2^{ij} = \frac{1}{K_2^{ij}}[-K_1^{ij}\delta\theta_1^{ij} + \delta m_1^{ij} + (K_1^{ij} + K_2^{ij})\delta\psi^i] \tag{A2}$$

$$\delta q_2^{ir} = -\delta q_1^{ir} \tag{A3}$$

$$\delta m_2^{ij} = A_{ij}L_i(-\delta\theta_1^{ij} + \delta\psi^i) + \left(\frac{K_5}{K_2}\right)^{ij}\delta m_1^{ij} \tag{A4}$$

where

$$\delta\psi^i = \frac{L^i}{C^{ir}}(A^{ir}\delta\theta_1^{ir} + \delta q_1^{ir} + \delta q_1^{ir} - B_1^{ir}\delta m_1^{ir} - \psi^i \delta P^{ir}) \tag{A5}$$

The elements of the field transfer matrix $\mathbf{G}^i$ as well the forcing vector $\mathbf{Q}^i$ of the present formulation, can be identified in Eqs. (A1)–(A4). Similarly, the system of equations represented in matrix form by Eq. (19) is

$$\delta v_1^{i+1,j} = \delta v_2^{ij} \tag{A6}$$

$$\delta\theta_1^{i+1,j} = \delta\theta_2^{ij} \tag{A7}$$

$$\begin{aligned}-\gamma_{i+1}\delta q_1^{i+1,r} = {}& (a^{i+1} - a^i)\delta\theta_2^{ir} + \gamma^i \delta q_2^{ir} + b_2^i \delta m_2^{ir} \\ & + b_1^{i+1}\delta m_1^{i+1,r} - + \sum_{j\neq r}[(A^{ij} - A^{i+1,j})\delta\theta_2^{ij} \\ & - B_2^{ij}\delta m_2^{ij} + B_1^{i+1,j}\delta m_1^{i+1,j}] - \delta r^1\end{aligned} \tag{A8}$$

$$\begin{aligned}-\delta m_1^{i+1,j} = {}& K_2^{I,J-1}\delta\theta_2^{i,j-1} + (K_5^{I,J-1} + K_1^{IJ})\delta_2^{ij} \\ & + K_{2\,2}^{IJ\,i,j+1} + m_2^{ij} - g^{rj}\end{aligned} \tag{A9}$$

where

$$\Gamma^i = \sum_{j\neq r} C^{ij} \tag{A10a}$$

$$\gamma^i = 1 + \frac{\Gamma^i}{C^{ir}} \tag{A10b}$$

$$a^i = \frac{A^{ir}}{C^{ir}}\Gamma^i \tag{A11a}$$

$$b_\alpha^i = \frac{B_\alpha^{ir}}{C^{ir}}\Gamma^i \tag{A11b}$$

and

$$\begin{aligned}\delta r^1 = {}& \sum_j [\delta r^{rj} + \psi^i \delta P^{ij} - \psi^{i+1}\delta P^{i+1,j}] \\ & + \gamma^{i+1}\psi^{i+1}\delta P^{i+1,r} - \gamma^i \psi^i \delta P^{ir}\end{aligned} \tag{A12}$$

The station transfer matrix $\mathbf{U}^I$ and the force vector $\mathbf{R}^I$ can be deduced from Eqs. (A6)–(A9). It is understood that moments at end 1 of member '$i + 1$', appearing on the right-hand side of Eq. (A8), are eliminated using Eq. (A9).

References

[1] Alvarez RJ, Birnstiel C. Inelastic analysis of multistory multibay frames. J Struct Div ASCE 1969;95(11):2477–503.

[2] Anderson D, Lok TS. An elastic–plastic hand method for unbraced rigid-jointed steel frames. In: Morris LJ, editor. Instability and Plastic Collapse of Steel Structures. Manchester: Granada, 1983. p. 104–9.

[3] Cohn MZ, Rafay T. Deformations of plastic frames considering axial forces. J Engng Mech Div Proc 1977;100(4):773–94.

[4] El-Zanaty MH, Murray DW. Nonlinear finite element analysis of steel frames. J Struct Engng ASCE 1983;109(2):353–68.

[5] Gharpuray V, Aristizabal-Ochoa JD. Simplified second-order elastic–plastic analysis of frames. J Comput Civ Engng ASCE 1989;3(1):47–59.

[6] Jennings A, Majid K. An elastic–plastic analysis by computer for framed structures loaded up to collapse. Struct Engnr 1965;43(12):407–12.

[7] Kassimali A. Large deformation analysis of elastic–plastic frames. J Struct Engng ASCE 1983;109(8):1869–86.

[8] King WS, White DW, Chen WF. Second-order inelastic analysis methods for steel-frame design. J Struct Engng ASCE 1992;118(2):408–28.

[9] Korn A. Effect of bowing on rectangular plane frames. J Struct Div Proc ASCE 1981;107(3):569–74.

[10] Korn A, Galambos TV. Behaviour of elastic–plastic frames. J Struct Div Proc ASCE 1968;94(5):1119–42.

[11] Lind NC. Iterative limit load analysis for tall frames. J Struct Div Proc ASCE 1964;90(2):103–29.

[12] Livesley RK, Chandler DB. Stability functions for structural frameworks. Manchester: Manchester University Press, 1956.

[13] NcNames BM, Lu L-W. Inelastic multistory frame buckling. J Struct Div Proc ASCE 1972;98(7):1613–31.

[14] Parikh B.P. Elastic–plastic analysis and design of unbraced multi-storey steel frames. Fritz Engineering Laboratory report no. 273.44, Lehigh University, Bethlehem, PA 1966.

[15] Syngellakis S, Kameshki ES. Elastic critical loads for plane frames by the transfer matrix method. J Struct Engng ASCE 1994;120(4):1140–57.

[16] Wood RH. The stability of tall buildings. Proc ICE 1958;11(1):69–102.

[17] Yau CY, Chan SL. Inelastic and stability analysis of flexibly connected steel frames by springs-in-series model. J Struct Engng ASCE 1994;120(10):2803–19.